Nanofibril Formation of Electrospun TiO$_2$ Fibers and its Application to Dye-Sensitized Solar Cells

Seong Mu Jo[a]; Mi Yeon Song[a]; Young Rack Ahn[ab]; Chong Rae Park[b]; Dong Young Kim[a]
[a] Optoelectronic Materials Research Center, Korea Institute of Science and Technology, Seoul, Korea [b] School of Materials Science and Engineering, Seoul National University, Seoul, Korea

PLEASE SCROLL DOWN FOR ARTICLE

Nanofibril Formation of Electrospun TiO₂ Fibers and its Application to Dye-Sensitized Solar Cells

SEONG MU JO,[1] MI YEON SONG,[1] YOUNG RACK AHN,[1,2] CHONG RAE PARK,[2] AND DONG YOUNG KIM[1]

[1]Optoelectronic Materials Research Center, Korea Institute of Science and Technology, Seoul, Korea
[2]School of Materials Science and Engineering, Seoul National University, Seoul, Korea

Electrospun TiO₂ nanofibers were employed to the quasi-solid state dye-sensitized solar cells with porous electrodes, which enhanced the penetration of viscous polymer gel electrolytes. The morphology of electrospun TiO₂ fibers was affected by the electrospinning parameters such as the types of polymers, the concentration of polymer and titanium(IV) propoxide (TiP), the ratio of TiP/PVAc. The TiO₂ fibers electrospun from poly(vinyl acetate) matrix formed the one-dimensionally aligned fibrillar morphology as an islands-in-a-sea structure. The new TiO₂ electrodes demonstrated that the photocurrent generation with polymer gel electrolytes was over 90% of the performance in a dye-sensitized solar cell with liquid electrolytes.

Keywords electrospinning, dye-sensitized solar cell, gel-electrolytes, TiO₂, nanofiber

Introduction

An electrospinning technique provided a simple, cost-effective approach for producing polymeric and inorganic nanofibers within a broad range of diameters, from tens of nanometers to a few micrometers according to the selection of the processing parameters. Several groups established that conventional sol-gel precursor solutions could be employed for electrospinning to provide a suitable route to composite and ceramic nanofibers (1–3). Recently, Xia et al. have tried to expand the possibility of electrospinning of TiO₂ fibers in various points of view such as fine diameter, hollow fibers, well-defined alignment, porous fiber morphology, etc. (4–8). In the present work, we found the fibrillar morphology using in-situ phase separation between polymer matrix and TiO₂ phases. The electrospinning parameters are discussed to control the TiO₂ fiber structures.

Nanofibers electrospun from conventional polymers have been applied to new fields such as nano filtration, tissue engineering, supporting materials for enzymes and catalysts based on nanopores and large surface area (9–11). To date however, only few electronic

application of electrospun inorganic nanofibers has been known due to the difficulties of constructing stable substrates for devices. We employed the electrospinning method to generate a TiO_2 nanofiber web, which we used as an electrode in a photoelectrochemical device, a so-called dye-sensitized solar cell (DSSC). In a typical DSSC, the triiodide/iodide redox couples in the liquid electrolyte regenerate the photo-oxidized dyes formed after releasing electrons to the conduction band of TiO_2 (12). However, the use of a liquid electrolyte may result in problems for the long-term stability and sealing of the DSSC. Several attempts used to quasi-solidify the liquid electrolyte by using polymer matrix or to replace the electrolytes with conductive organic materials as a hole transport layer of the cells (13, 14). In those cases, imperfect filling of the cells cased the insufficient conversion efficiencies of the solid cells compare to those using a liquid electrolyte (15). In this work, the TiO_2 nanofibers were employed to a quasi-solid state dye-sensitized solar cell with porous electrodes which enhanced the penetration of viscous polymer gel electrolyte.

Experimental

Electrospinning of TiO$_2$ Fibers

Electrospinning solutions were prepared from polymers such as polystyrene (PS), poly-(methyl methacrylate) (PMMA) and poly(vinyl acetate) (PVAc) in dimethyl formamide (DMF) with stirring (Figure 1). PS, PMMA and PVAc were purchased from Aldrich Co. A certain volume of titanium (IV) propoxide (TiP) was added into the polymer solutions under stirring. Acetic acid was added to this solution to get a transparent yellow solution with vigorous stirring over 2 h. A schematic diagram of electrospinning equipment is shown in Figure 2. The solution was loaded into a syringe equipped with a 24 gauge silver-coated needle. The needle was connected to a high voltage power supply (Bertan Model 205B-50R). The electric voltage of 15 kV was applied between the metal orifice and the ground state at a distance of ca. 10 cm. The spinning rate was controlled by the syringe pump (KD Scientific model 220) attached to the orifice.

Characterization Techniques

Viscosity measurement of electrospinning solutions was performed with a dynamic viscometer at 30°C (DV-II+ Pro Digital Viscometer, Brookfield). The molecular weight of polymers was determined using gel permeation chromatography (GPC, Jasco RI-2031)
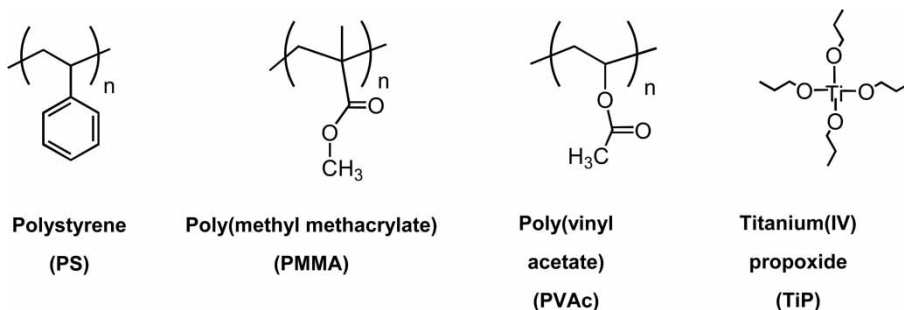

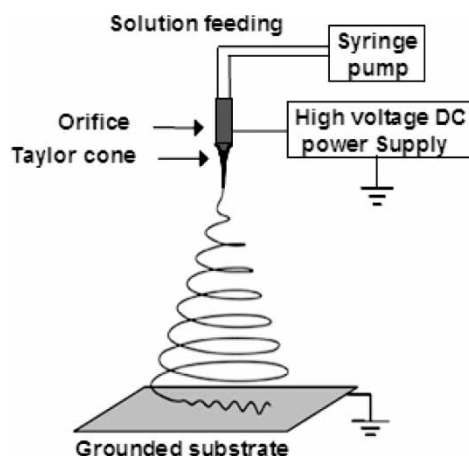**Figure 1.** Structures of polymers and TiP for electrospinning.

Figure 2. Schematic diagram of an electrospinning equipment.

with polystyrene standards. Tetrahydrofuran (THF) was used as the eluent for GPC analysis. The morphology and diameter of the fibers were determined using the field emission scanning electron microscopy (FE-SEM, JSM-6330F, JEOL). The detailed morphology of the fibers was also examined by the transmission electron microscopy (TEM, CM-20, Philips) and the selected area electron diffraction (SAED). A drop of TiO$_2$ fiber suspension in ethanol was mounted onto a carbon-coated 400-mesh Cu grid.

Device Fabrication and Characterization

TiO$_2$ fibers were electrospun directly onto a SnO$_2$:F coated glass substrate (FTO, 10 cm × 10 cm, TEC-15, Pilkington) from mixed solution containing 3 g of PVAc (MW 850,000 g/mol) and 6 g of TiP with 2.4 g acetic acid as a catalyst in DMF (37.5 mL). In order to form a uniform thickness in a large area, the nozzle and the substrate were placed on the motion control system with a microprocessor. Electrospun TiO$_2$ web was treated with THF vapor in a closed chamber for 1 h prior to calcination. The calcination was carried out stepwise at each temperature (duration in min) as 100 (15); 150 (15); 325 (5); 450°C (30) in air. In order to prepare a DSSC device, the calcined TiO$_2$ web electrode was immersed overnight in ethanol containing 3×10^{-4} M RuL$_2$(NCS)$_2$ (L = 2,2′-bipyridyl-4,4′-dicarboxylic acid) (N3, Solaronix). The dye-absorbed TiO$_2$ electrode was rinsed with ethanol and dried under the nitrogen flow. The liquid electrolyte was consisted of 0.6 M 1-hexyl-2,3-dimethyl-imidazolium iodide (C6DMIm), 0.05 M iodine (I$_2$), 0.1 M lithium iodide (LiI) and 0.5 M 4-tert-butylpyridine dissolved in 3-methoxyacetonitrile. Pt-sputtered SnO$_2$:F glass was used as a counter electrode. The DSSC containing a polymer gel electrolyte was also characterized using a mixture of poly(vinylidene fluoride-*co*-hexafluoropropylene) (PVDF-HFP) (Kynar 2801, 0.13 g), C6DMIm (0.13 g) and I$_2$ (0.008 g) in propylene carbonate (0.75 g) and ethylene carbonate (0.5 g). The typical active area of the cell was 0.16 cm^2. The J-V characteristics were measured using a Keithley SMU 2400 under 100 mW/cm^2 irradiation from a Xe lamp (Oriel, 300 W) with a global AM1.5 filter for solar spectrum simulation. The light was calibrated using a reference solar cell (Fraunhofer Institute) and calibrated photodiode (Melles-Griot, Model 13PEM001).

Results and Discussion

Electrospinning of TiO₂ Fibers

The electrospinning of inorganic fibers was processed using the mixed solution of sol-gel precursors with viscous polymer binders in organic solvents. The role of polymer binder increases the viscosity to form fibers during the electro-spinning process and to control the morphology of spun fibers. The electro-spinning process is similar to an electro-spraying technique, which produces fine particles under high electrical fields without polymer binders. The fiber formation of inorganic-organic hybrid materials is a complicated process including a sol-gel transformation reaction and solidification. At the beginning of electro-spinning, a fiber stream from a positive charged Taylor cone at nozzle starts the sol-gel transformation reaction with ambient moistures followed by phase separation between organic polymer and inorganic phases. Therefore, the miscibility problem is one of the important parameters to control the electrospun fibers. In this study, three different polymers such as polystyrene (PS), poly(methyl methacrylate) (PMMA) and poly(vinyl acetate) (PVAc) were applied to optimize the properties of electrospun TiO₂ fibers for the electrodes of dye-sensitized solar cells.

Polystyrene

Polystyrene (PS, Aldrich, MW 350,000 g/mol) was electrospun from the mixed solution of 0.25 g/mL in DMF including 0.19 g/mL of TiP and catalytic amount of acetic acid. The morphology of electrospun TiO₂ fibers was shown in Figure 3 after calcination at 450°C for 30 min in air. PS in as-spun fibers was removed completely during calcination. The
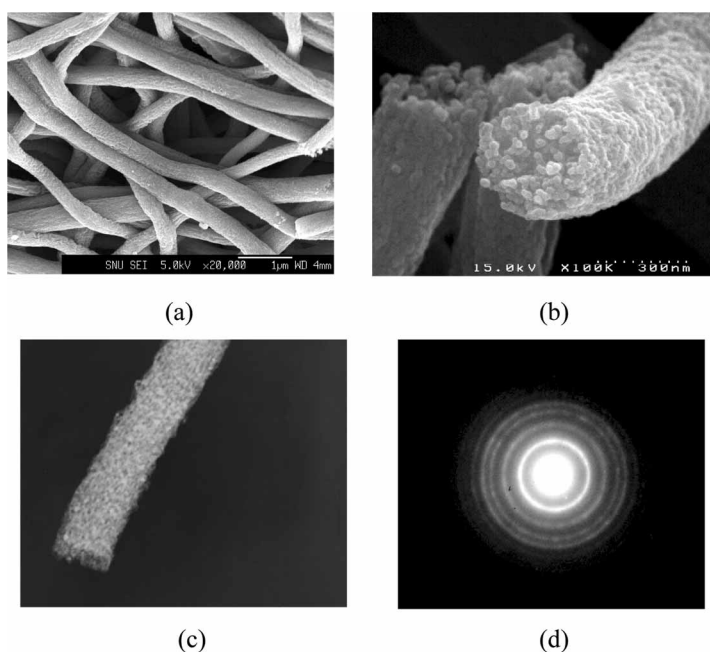

(a)

(b)

(c)

(d)

Figure 3. Morphology of TiO₂ fibers electrospun from PS solution: SEM (a and b), TEM (c), and SAED (d).

fiber diameters were ca. 300 nm after calcination. Each fiber was composed of TiO_2 particles in size of 30 nm as shown in Figure 3(b). The particle formation in solidification process occurred as a result of fast phase separation due the immiscibility between PS and TiO_2 phases. The fiber morphology was fixed at the early stage without further changes. The cross-section in Figure 3(b) shows the same morphology at inner parts and surface, which was also confirmed from TEM image in Figure 3(c). The TiO_2 particles formed the anatase structure after calcination and the SAED pattern in Figure 3(d) shows the clear diffraction rings which are related to each anatase crystal surface. The SAED follows a typical powder pattern in which the crystal arrangement is randomly oriented.

Poly(methyl methacrylate)

TiO_2 fibers were electrospun from the mixed solution of poly(methyl methacrylate) (PMMA, Aldrich, MW 996,000 g/mol) with 0.19 g/mL of TiP in DMF. The fiber morphology are shown in Figure 4. The fiber diameter was ca. 500 nm and the size distribution
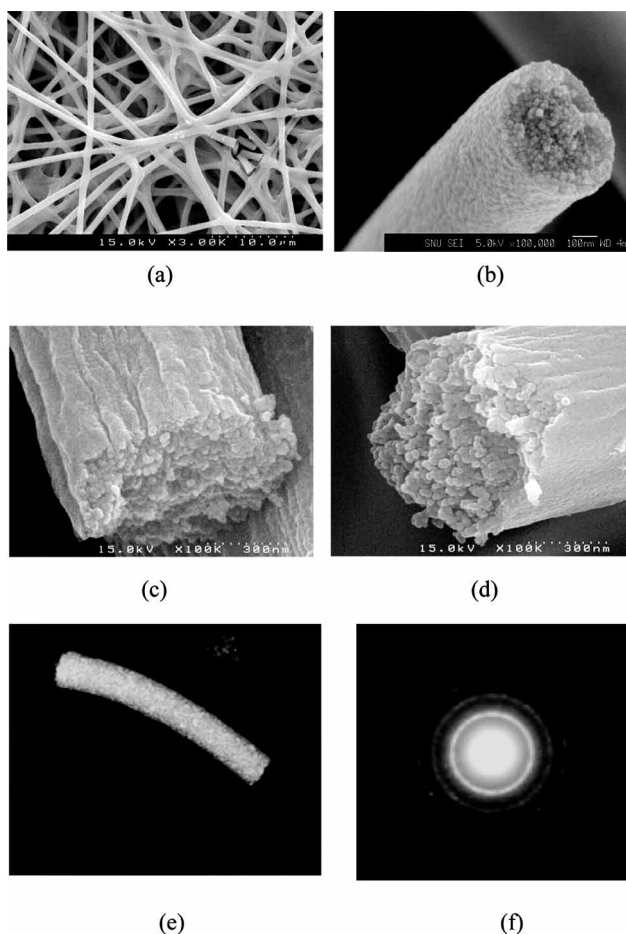

(a)

(b)

(c)

(d)

(e)

(f)

Figure 4. Morphology of TiO_2 fibers electrospun from PMMA solution containing TiP (0.19 g/mL): (a) web, (b) PMMA 0.10 g/mL, (c) 0.12 g/mL, (d) 0.14 g/mL, (e) TEM, and (f) SAED.

was not uniform compared to that of the PS matrix. PMMA has the better miscibility to the TiP precursor than PS due to the carbonyl functional group which increases the molecular interactions. The effects of polymer concentration on the fiber morphology were studied with three different spinning solutions containing 0.10, 0.12, and 0.14 g/mL of PMMA. The structures of fibers from different solutions after the calcinations at 450°C are shown in Figure 4(b), 4(c) and 4(d), respectively. TiO$_2$ fibers electrospun from 0.10 g/mL of PMMA were composed of fine particles as shown in Figure 4(b), which were smaller than those in PS matrix. As increased concentration to 0.12 g/mL of PMMA, the surface morphology was different to inner part as shown in Figure 4(c). The surface formed the smooth clading sheath and the inner part was filled with particles, which were larger than those from 0.10 g/mL. There were large wrinkles at the sheath in the spinning direction. The sol-gel transformation and phase separation were affected by the concentration of the polymer matrix and the process at the surface of fibers was different from that in the inner part of fibers. The structural difference in the sheath and core became clearer at the concentration of 0.14 g/mL as shown in Figure 4(d). The TEM and SAED pattern in Figure 4(e) and 4(f) were similar to those from the PS matrix, which revealed the powder pattern of randomly oriented anatase crystal.

Poly(Vinyl Acetate)

Poly(vinyl acetate) (PVAc) is known to have good miscibility to the TiP sol-gel precursor. In this study, the effects of the molecular weight, the concentration and the ratio between PVAc and TiP were investigated in detail to optimize the fiber structure in an application to dye-sensitized solar cells. The viscosity of spinning solution affects the fiber diameter, as well as the morphology. One of the methods to change the viscosity is to vary the concentration of polymers. However, it is very difficult to control the viscosity simply with concentration, since TiP as in the organic component also affects the final structure and property of electrospun fibers after calcination.

TiO$_2$-PVAc composite fibers were electrospun from the various compositions as seen in Table 1 with two different molecular weights of PVAc, MW 500,000 g/mol (L-PVAc) and 850,000 g/mol (H-PVAc). The L-PVAc was purchased from Aldrich Co. and the H-PVAc was synthesized using bulk radical polymerization to obtain high molecular weight polymers. The viscosity of the spinning solution decreased after adding TiP and acetic acid as a catalyst due to the hydrolysis of PVAc as shown in Table 1. The initial

Table 1
Composition of the spinning solutions

	L-PVAc (500,000 g/mol)			H-PVAc (850,000 g/mol)		
	(a)	(b)	(c)	(d)	(e)	(f)
PVAc (g/mL in DMF)	0.08	0.19	0.19	0.08	0.08	0.08
TiP (g/mL in DMF)	0.19	0.40	0.19	0.09	0.19	0.42
TiP/PVAc ratio (wt.)	2.38	2.10	1.00	1.12	2.38	5.25
Viscosity (cP) (PVAc solution only)	172	4,180			1,560	
(With TiP and acetic acid)	112	718			788	

viscosity of the composition in Table 1(a) decreased from 172 cP to 112 cP after adding the sol-gel precursor. The viscosity of the spinning solution with 0.19 g/mL of L-PVAc in Table 1(b) changed from 4,180 cP to 768 cP. On the other hand, the viscosity of the spinning solution with H-PVAc (Table 1(e)) decreased less than that of L-PVAc.

Figure 5 shows the morphology of TiO$_2$ fibers electrospun from the solution as the composition in Table 1 after calcinations, in which all the PVAc were removed at 450°C. The TiO$_2$ fibers from the solution of 0.08 g/mL L-PVAc and 0.19 g/mL TiP (Table 1(a)) showed the diameter of ca. 100 nm as shown in Figure 5(a) which was smaller than the fibers of other compositions in the range of 300–500 nm. The lower the viscosity of the spinning solution, the smaller the fiber diameter obtained. The fibers in Figure 5(a) were composed of particles which had an elongated shape instead of a spherical one. There was no difference between the surface and inner part of the fibers. These fibers could not be applied to an electrode for DSSC due to the poor adhesion to substrates.
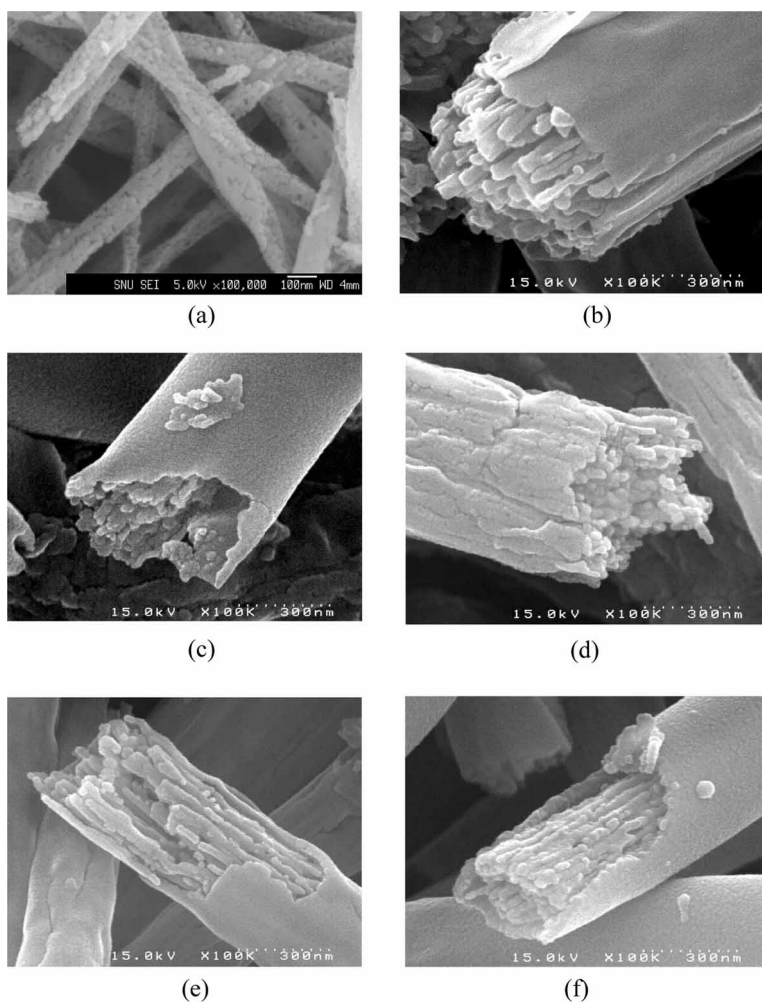

Figure 5. Morphology of TiO$_2$ fibers electrospun from PVAc solution containing TiP with the composition in Table 1.

When the polymer concentration increased to 0.19 g/mL as Table 1(b) with maintaining the ratio of TiP/PVAc as 2.1, interestingly, the morphology showed the sheath-and-core structure as shown in Figure 5(b). The cross-section of fibers also showed an islands-in-a-sea structure in which the bundle of fibrils was surrounded by the clading sheath. The *in situ* formation of the islands-in-a-sea morphology has not been found yet as a result of the phase separation of two components in the electrospinning process. The fibril had a diameter of ca. 20 nm and oriented to the fiber direction.

The ratio of TiP/PVAc affected the fiber morphology due to the different TiO_2 contents after removing PVAc at calcination. The fiber from the solution of Table 1(c) as the ratio of 1.0 showed a similiar diameter to the fiber with the concentration of PVAc, 0.19 g/mL (Table 1(b)). However, the fibril density decreased with increasing the PVAc content as shown in Figure 5(c) and the surface became rough compared to the fibers in Figure 5(b).

The spinning solution with the high molecular weight H-PVAc formed fibers even in a low concentration of PVAc of 0.08 g/mL. The fiber morphology with the different ratio of TiP/PVAc was shown in Figure 5(d), 5(e), and 5(f) for 1.12, 2.38 and 5.25, respectively. The fiber of the ratio, 1.12 formed the fibrillar structure, but the cracks were found at the surface because of a relatively large content of PVAc. As the ratio increased, the surface became smoother, and the sheath-and-core structure formed were similar to the fibers with L-PVAc. The fibrils in the fiber from the ratio of 5.25 were densely packed with higher TiO_2 contents.

The fibril structure of TiO_2 fibers from the PVAc matrix clearly showed the oriented crystal structure as shown in Figure 6 where the SAED pattern revealed the diffraction spots different from the ring patterns in the cases of PS and PMMA. The ratio of TiP/PVAc in the spinning solution was one of the most important parameters to control the fibril morphology and the optimum ratio was ca. 2.0.

The Mechanism of Fibril Formation

The structure of TiO_2 fibers electrospun from the mixed solution of TiP and polymers was affected by the several parameters such as the types of polymer matrix, the concentration
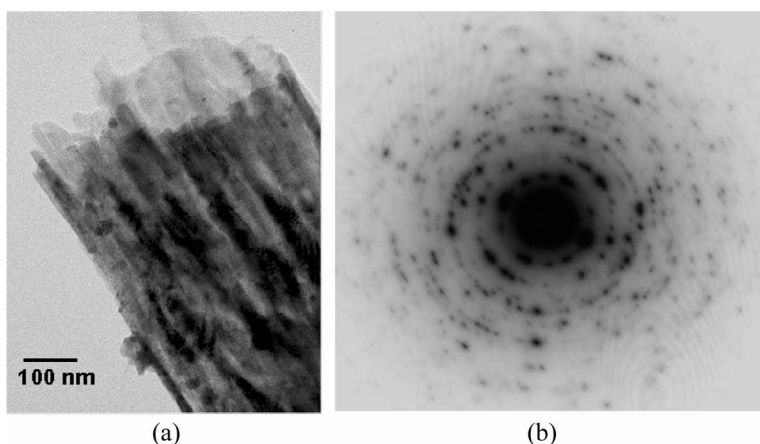

(a)	(b)

Figure 6. TEM (a) and SAED pattern (b) of TiO_2 fiber electrospun from PVAc and TiP solution (Table 1(e)).

of polymer and TiP, the ratio of TiP/PVAc, etc. In particular, the electrospinning process of metal oxide fibers is more complicated due to the sol-gel transformation reaction during the spinning. In this section, we propose the mechanism of the fibril formation and the sheath-and-core structure of electrospun TiO_2 fibers. The fiber formation in the electrospinning process is considered as the following factors: (a) the sol-gel transformation reaction with ambient moistures, (b) the concentration change after evaporation of solvents, (c) the temperature lowering and condensation of moisture due to the heat of evaporation, (d) the dynamic phase separation phenomena in terms of miscibility, (e) the stability of separated phases, (f) the mechanical transformation, (g) the solidification process, etc. It is very difficult to understand all the phenomena separately, since the process is carried out dynamically in a short time. The mechanism for the electrospun TiO_2 fibers is suggested simply in three steps as illustrated in Figure 7.

At first, the TiP precursor starts the sol-gel transformation from the reaction with ambient moistures. The spinning solution contains the TiO_2 sol from the pre-reaction with acetic acids in polymer solution before spinning and the sol-state is converted rapidly to the gel-state. At this stage, the solvent is evaporated with increased surface area due to the decrease in diameter of flow stream. The miscible equilibrium state in spinning solution becomes unstable thermodynamically due to the concentration fluctuation of each component. The phase separation and solidification of the TiO_2 phase occur abruptly in the immiscible system such as in the PS matrix resulting in particle formation as mentioned in the previous section. On the other hand, the miscible system such as PVAc system, the phase separation carries out slowly and the TiO_2-rich, as well as PVAc-rich domains, co-existed to allow the domain elongation in liquid phases. Also, the lowered temperature of the surface accelerates the gel transformation due to the condensation of moisture resulting in the sheath formation of TiO_2 fibers. The solidified fiber forms the sheath-and-core structure with fibrils as the islands-in-a-sea morphology. The detailed density and size of fibrils are affected by the ratio of TiP/PVAc, as well as the viscosity of the spinning solution.

Dye-Sensitized Solar Cells

One of the problems with electrospun inorganic electrodes is their poor adhesion to substrates after calcinations in which the binder polymers are removed. The TiO_2 web was found to be peeled off from substrates, so in this form, it cannot be used in electronic
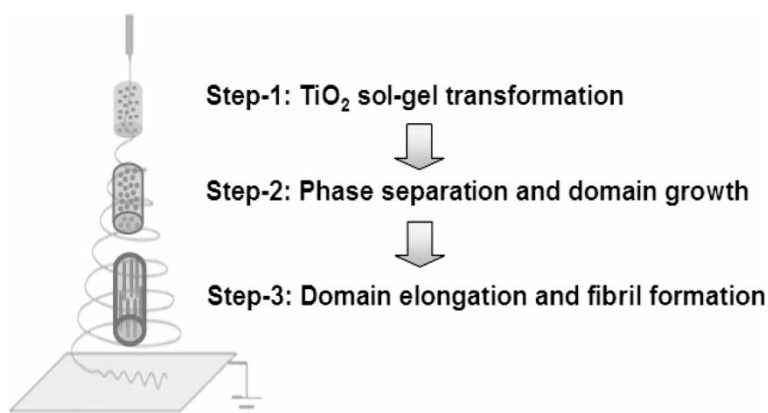

Figure 7. The suggested mechanism of the nanofibril formation in electrospun TiO_2 fibers.

devices as shown in Figure 8(a). In this study, we prepared a very stable TiO_2 electrode by electrospinning the fibers directly onto an FTO substrate and pretreating them prior to calcination. The PVAc and TiO_2 composite fibers were treated with solvent vapor in a closed chamber. Some PVAc were dissolved from the electrospun composite fibers and produces a thin film of PVAc over the fiber web. In Figure 8(c), it can be seen that the untreated fibers are separated from each other. This separation results in the delamination of the untreated TiO_2 web from the substrate during calcination. The pretreated TiO_2 fibers were found to be interconnected, and after heat treatment, the TiO_2 electrode retained the porous structure of the TiO_2 web, as shown in Figure 8(b) and 8(d).

Figure 9 presents the photocurrent density-voltage (J-V) curves for cells based on the electrospun TiO_2 nanofiber electrodes (ca. 20 μm in thickness) in combination with liquid or polymer gel electrolytes. The photovoltaic characteristics were analyzed by the following Equations (1) and (2):

$$FF = \frac{V_{max} \times J_{max}}{V_{oc} \times J_{sc}} \tag{1}$$

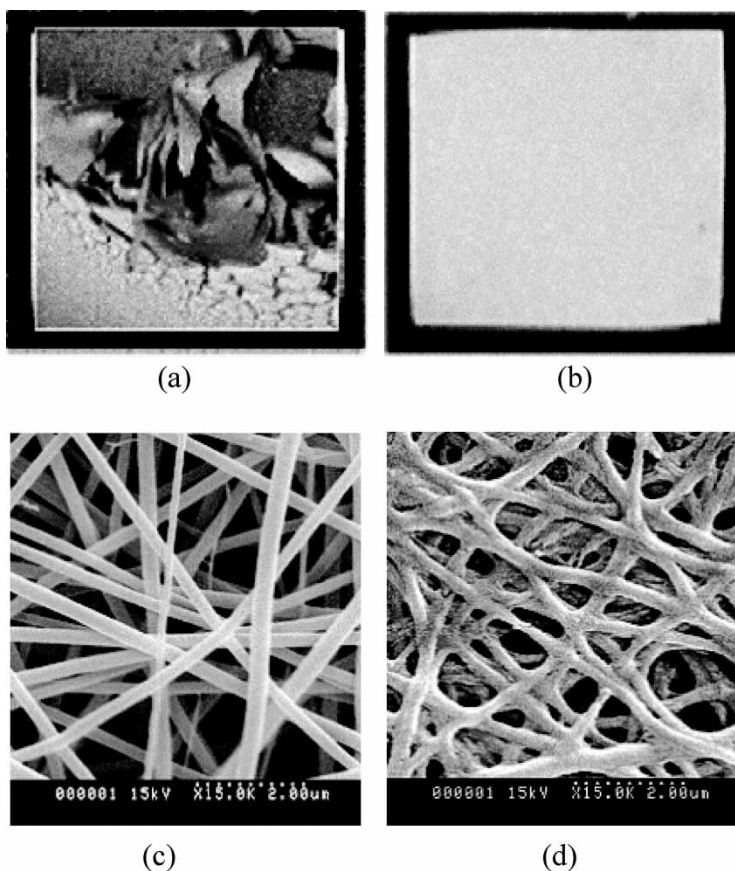$$\eta\ (\%) = \frac{V_{oc} \times J_{sc} \times FF}{I_v} \times 100 \tag{2}$$

Figure 8. Electrospun TiO_2 electrodes for DSSCs without (a and c) and with pre-treatment (b and d).
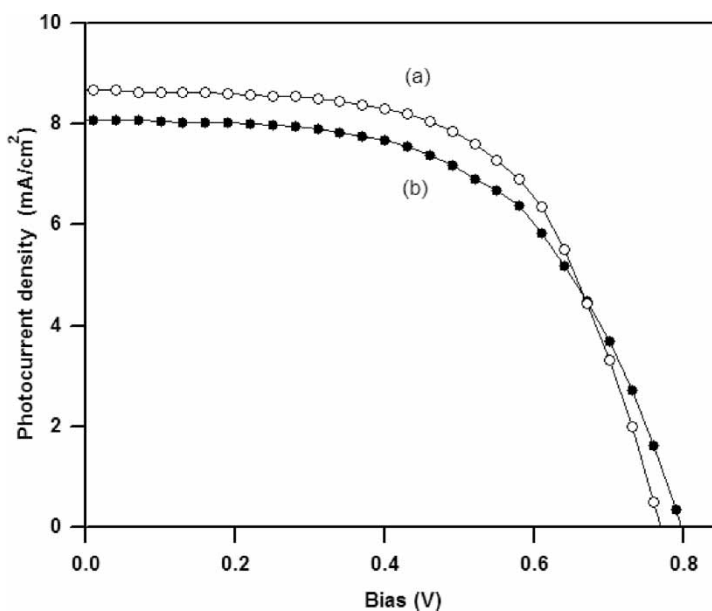
Figure 9. Photocurrent density-voltage characteristics of DSSCs with electrospun TiO$_2$ electrodes with liquid (a) and gel (b) electrolytes. All the measurements were carried out using the global AM1.5 solar simulator at $100 \, \text{mW/cm}^2$.

where the fill factor (FF) is the maximum power delivered to an external load, calculated from the short-circuit current density (J$_{sc}$) and the open-circuit voltage (V$_{oc}$). The overall conversion efficiency (η) is normalized by the intensity of incident light (I$_v$).

The device containing liquid electrolyte was found to have the following characteristics, as shown in Figure 9(a): V$_{oc}$ (0.77 V), J$_{sc}$ (8.67 mA/cm^2), FF (0.60) and η (4.01%). The device containing polymer gel electrolyte was also tested with the same electrospun TiO$_2$ electrode. For the gel electrolyte device, J$_{sc}$ and η were found to be 8.07 mA/cm^2 and 3.80%, respectively, as shown in Figure 9(b). The overall η and J$_{sc}$ obtained for the gel electrolyte system were 94.8% and 93%, of the values for the liquid electrolyte system, respectively. The success of the application of the electrospun TiO$_2$ electrode in a DSSC should be judged by the degree of penetration of the highly viscous gel electrolyte into the porous space of the TiO$_2$ layer. The well-aligned 1-D morphology of the TiO$_2$ fibers may also contribute to better charge conduction, because of their reduced grain boundaries compared to those of the sintered nanoparticles.

Conclusions

In summary, we have successfully demonstrated that electrospun TiO$_2$ electrodes provide a new alternative to the use in DSSCs of conventional electrodes consisting of nanocrystalline TiO$_2$ particles because of the enhanced penetration of the polymer gel electrolyte. The morphology of electrospun TiO$_2$ fibers were affected by the electrospinning parameters such as the types of polymers, the concentration of polymer and TiP, the ratio of TiP/PVAc. The electrospun TiO$_2$ fibers from PVAc matrix formed the fibrillar structure with an islands-in-a-sea morphology. The performance of the gel electrolyte

system with an electrospun electrode was found to be greater than 90% of an equivalent liquid electrolyte system. The electrospun TiO_2 fibers have a 1-D ordered fibrillar structure and the direct production of stable electrodes with the electrospinning method can give them new features and applications in electronic devices.

References

1. Madhugiri, S., Sun, B., Smirniotis, P.G., Ferraris, J.P., and Balkus, K.J. (2004) Electrospun Mesoporous Titanium Dioxide Fibers. *Micro. Meso. Mater.*, 69: 77–83.
2. Ding, B., Kim, H., Kim, C., Khil, M., and Park, S. (2003) Morphology and Crystalline Phase Study of Electrospun TiO_2-SiO_2 Nanofibres. *Nanotechnology*, 14: 532–537.
3. Guan, H., Shao, C., Chen, B., Gong, J., and Yang, X. (2003) A Novel Method for Making CuO Superfine Fibres Via a Electrospinning Technique. *Inorg. Chem. Comm.*, 6: 1409–1411.
4. Li, D., Wang, Y., and Xia, Y. (2004) Electrospinning Nanofibers as Uniaxially Aligned Arrays and Layer-by-Layer Stacked Films. *Adv. Mater.*, 16: 361–366.
5. Li, D. and Xia, Y. (2004) Electrospinning of Nanofibers: Reinventing the Wheel? *Adv. Mater.*, 16: 1151–1170.
6. Li, D. and Xia, Y. (2003) Fabrication of Titania Nanofibers by Electrospinning. *Nano Lett.*, 3: 555–560.
7. Li, D. and Xia, Y. (2004) Direct Fabrication of Composite and Ceramic Hollow Nanofibers by Electrospinning. *Nano Lett.*, 4: 933–938.
8. Li, D., Wang, Y., and Xia, Y. (2003) Electrospinning of Polymeric and Ceramic Nanofibers as Uniaxially Aligned Arrays. *Nano Lett.*, 3: 1167–1171.
9. Subbiah, T., Bhat, G.S., Tock, R.W., Parmeswaran, S., and Ramkumar, S.S. (2005) Electrospinning of Nanofibers. *J. Appl. Poly. Sci.*, 96: 557–569.
10. Yoshimoto, H., Shin, Y.M., Terai, H., and Vacanti, J.P. (2003) A Biodegradable Nanofiber Scaffold by Electrospinning and its Potential for Bone Tissue Engineering. *Biomaterials*, 24: 2077–2082.
11. Jia, H., Zhu, G., Vugrinovich, B., Kataphinan, W., Reneker, D.H., and Wang, P. (2002) Enzyme-Carrying Polymeric Nanofibers Prepared via Electrospinning for Use as Unique Biocatalysts. *Biotechnol. Prog.*, 18: 1027–1032.
12. O'Regan, B. and Grätzel, M.A. (1991) Low-Cost, High Efficiency Solar Cell Based on Dye-Sensitized Colloidal TiO_2 films. *Nature*, 353: 737–739.
13. Kubo, W., Kambe, S., Nakade, S., Kitamura, T., Hanabusa, K., Wada, Y., and Yanagida, S. (2003) Photocurrent-Determining Processes in Quasi-Solid-State Dye-Sensitized Solar Cells Using Ionic Gel Electrolytes. *J. Phys. Chem. B*, 107: 4374–4381.
14. Schmidt-Mende, L., Zakeeruddin, S., and Grätzel, M. (2005) Efficiency Improvement in Solid-State-Dye-Sensitized Photovoltaics with an Amphiphilic Ruthenium-Dye. *Appl. Phys. Lett.*, 86: 013504.
15. O'Regan, B., Lenzmann, F., Muis, R., and Wienke, J. (2002) A Solid-State Dye-Sensitized Solar Cell Fabricated with Pressure-Treated P25-TiO_2 and CuSCN: Analysis of Pore Filling and IV Characteristics. *Chem. Mater.*, 14: 5023–5029.